

# Collective modes of a two-dimensional Fermi gas at finite temperature

Brendan C. Mulkerin,<sup>1</sup> Xia-Ji Liu,<sup>1</sup> and Hui Hu<sup>1</sup>

<sup>1</sup>*Centre for Quantum and Optical Science, Swinburne University of Technology, Melbourne 3122, Australia.*  
(Dated: July 29, 2021)

In this work we examine the breathing mode of a strongly interacting two-dimensional Fermi gas and the role of temperature on the anomalous breaking of scale invariance. By calculating the equation of state with different many-body  $T$ -matrix theories and the virial expansion approach, we obtain a hydrodynamic equation of the harmonically trapped Fermi gas (with trapping frequency  $\omega_0$ ) through the local density approximation. By solving the hydrodynamic equation we determine the breathing mode frequencies as functions of interaction strength and temperature. We find that the breathing mode anomaly depends sensitively on both interaction strength and temperature. In particular, in the strongly interacting regime we predict a significant down-shift of the breathing mode frequency, below the scale invariant value of  $2\omega_0$  for temperatures of order the Fermi temperature.

PACS numbers: 03.75.Hh, 03.75.Ss, 67.85-d

## I. INTRODUCTION

Fermi gases in two dimensions are of significant importance in understanding many-body systems [1, 2]. Ultracold atomic Fermi gases near a Feshbach resonance offer a new type of strongly interacting quantum system, where experimentalists have precise control over almost all the physical properties of the system, such as interaction strength, particle number, and dimension. Interactions are described through a zero-range delta-potential, which in two dimensions is known to be an example of a quantum anomaly [3]. The classical symmetry of a system interacting through a delta potential in two dimensions is scale invariant under the transformation  $\mathbf{r} \rightarrow \lambda \mathbf{r}$ , and an analysis of the scattering properties of a quantum system shows that it is divergent and must be regularized [4–6]. This well known regularization introduces a new length scale, the two-dimensional (2D) scattering length  $a_{2D}$ , and the scale invariance of the classical theory has been broken. The quantum anomaly can be seen through the breathing mode of trapped ultracold gases [7, 8]. Harmonically trapped gases possess a hidden  $SO(2,1)$  symmetry [9], which excites a breathing mode at a frequency of  $\omega = 2\omega_0$ , where  $\omega_0$  is the frequency of the trapping potential. The breaking of scale invariance through the delta-potential interaction will excite a breathing mode, whose frequency is dependent on the regularized 2D scattering length,  $a_{2D}$ . The advent of 2D ultracold gases realized for fermions [10–14] and bosons [15–18] are ideal systems for measuring the breathing mode and the anomalous breaking of scale invariance.

In Fermi gas experiments the breathing mode and anomalous corrections have been studied by Refs. [19, 20], where the breathing mode frequency shifts - away from the scale invariance value of  $2\omega_0$  - were of order a few percent, but the errors within the experiment made the observation of the anomaly inconclusive. It was argued that at the temperature of the experiment,  $T/T_F \simeq 0.42$ , the anomaly was damped, and that we would expect at lower temperatures the frequency shifts of the breathing

mode to be more pronounced. Theoretically the breathing mode of harmonically trapped 2D gases has been extensively studied at zero temperature [21–23] using quantum Monte Carlo to determine the equation of state [24], and at finite temperature [25] with the high-temperature virial expansion up to the second order. In all cases, the breathing mode frequency can be calculated through a variational approach of the hydrodynamic equations [26–30]. At  $T = 0$  the breathing mode shifts from the scale invariant value found by Refs. [21, 23] are positive for all interaction strengths at the crossover from a Bose-Einstein condensate (BEC) to a Bardeen-Cooper Schrieffer (BCS) superfluid, and in the strongly interacting regime they can reach approximately 10% of the scale invariant result. The virial expansion analysis at finite temperature done by Ref. [25] focused on the comparison to the experiment of Ref. [19] and did not examine the role of temperature on the breathing mode. To address the temperature effect, it necessarily requires sufficient knowledge about the equation of state of a strongly interacting 2D Fermi gas at finite temperature, which unfortunately remains a grand challenge both experimentally [12, 14] and theoretically [31].

In Bose gas experiments [15, 16] the breathing mode was measured for only weakly interacting systems where the system appears to be scale invariant and robust to temperature, and no breathing mode anomaly has been observed. Theoretically, it was found that there is a temperature dependence of the breathing mode in the weakly interacting regime [32], however it should be noted that this deviation is not due to the breaking of scale invariance and is a result of small deviations from the effective harmonic trapping potential.

In this work, we aim to present a systematic investigation of the finite-temperature breathing mode of a strongly interacting 2D Fermi gas, by gathering the most advanced knowledge of the 2D homogeneous equation of state developed in some recent theoretical works [31, 33–39]. At low temperature, we consider the non-self-consistent pair-fluctuation theory by Nozières and

Schmitt-Rink (NSR) [40, 41] and the self-consistent  $T$ -matrix approximation [42] in the normal state, taking the effects of pairs explicitly into account. In the high temperature and weakly interacting regimes we employ the virial expansion [43] to second and third order [33, 36]. Using the local density approximation with the homogeneous equation of state we calculate the collective modes of a trapped system using a variational approach at a given trap temperature and interaction strength [29]. We find theoretically that the breathing mode anomaly is temperature dependent as well as interaction dependent. In the weakly interacting BCS regime, the breathing mode is reduced towards the scale invariant result of  $2\omega_0$ , as temperature is increased. In the strongly interacting regime and in the high temperature regime, well above the superfluid temperature  $T_c$ , the breathing mode lowers below the scale invariant value, indicating the importance of pair formation at high temperature.

This paper is organized as follows. In Sect. II we introduce a diagrammatic approach to the pressure equation of state and the virial expansion. In Sect. III we introduce the variational formalism for ultracold gases and derive the thermodynamic properties for the calculation of the breathing mode. In Sect. IV we discuss the results of the breathing mode. We present a brief conclusion and outlook in Sect. V. The two appendices (Appendix A and Appendix B) are devoted to the details of variationally solving the hydrodynamic equation.

## II. THEORY

In this section, for self-containedness we review the theories of a strongly interacting Fermi gas in two dimensions [31]. At low temperature, we focus on the non-self-consistent NSR approach, since it provides the easiest way to take into account strong pair-fluctuations in 2D, with the most stable numerical outputs for the equation of state. At high temperature, we introduce a Páde approximation to re-organize the virial expansion series, which may extend the applicability of virial expansion towards the low-temperature regime. It is worth noting that for a 2D Fermi gas at finite temperature (i.e.,  $0 < T \lesssim T_F$ ), all the strong-coupling theories so far are *qualitative* only. It is notoriously difficult to carry out numerically accurate quantum Monte Carlo simulations at finite temperature due to the Fermi sign problem, even in the normal state [44].

### A. Many-body $T$ -matrix theories

In order to explore the finite temperature behavior of 2D Fermi gases at the BEC-BCS crossover, following NSR we consider the contribution of pairing fluctuations to the thermodynamic potential for a given temperature  $T$  and binding energy  $\varepsilon_B = \hbar^2/(Ma_{2D}^2)$  through the functional integral formulation, which has been ex-

tensively studied in both two and three dimensions in the normal and superfluid states [34, 39, 45–51]. The equation of state is found through the thermodynamic potential  $\Omega = -k_B T \ln \mathcal{Z}$  where the partition function is  $\mathcal{Z} = \int \mathcal{D}[\psi_\sigma, \bar{\psi}_\sigma] e^{-S[\psi_\sigma, \bar{\psi}_\sigma]}$ , and  $\psi_\sigma$  and  $\bar{\psi}_\sigma$  are independent Grassmann fields representing fermionic species for each spin degree of freedom,  $\sigma = \uparrow, \downarrow$ , of equal mass  $M$ . The partition function is defined through the action

$$S = \int_0^{\hbar\beta} d\tau \left[ \int d\mathbf{r} \sum_\sigma \bar{\psi}_\sigma(x) \partial_\tau \psi_\sigma(x) + \mathcal{H} \right], \quad (1)$$

and the single channel Hamiltonian given by

$$\mathcal{H} = \bar{\psi}_\sigma(x) \mathcal{K} \psi_\sigma(x) - U_0 \bar{\psi}_\uparrow(x) \bar{\psi}_\downarrow(x) \psi_\downarrow(x) \psi_\uparrow(x), \quad (2)$$

where  $\mathcal{K} = -\hbar^2 \nabla^2 / (2M) - \mu$ ,  $\beta = (k_B T)^{-1}$ ,  $\mu$  is the chemical potential, and  $x = (\mathbf{x}, \tau)$  for position  $\mathbf{x}$  and imaginary time  $\tau$ . We take a contact interaction with  $U_0 > 0$ , which has known divergences and can be fixed through renormalizing in terms of the bound state energy via the relation,

$$\frac{1}{U_0} = \sum_{\mathbf{k}} \frac{1}{2\epsilon_{\mathbf{k}} + \varepsilon_B}, \quad (3)$$

where  $\epsilon_{\mathbf{k}} = \hbar^2 \mathbf{k}^2 / (2M)$ . Using the Hubbard-Strantonovich transformation to write the action in terms of the bosonic field and integrating out the fermionic Grassmann fields, at the Gaussian fluctuation level in the normal state we obtain the thermodynamic potential,

$$\Omega = \Omega_0 - \sum_{\mathbf{q}, \nu_n} \ln [-\Gamma_0^{-1}(\mathbf{q}, i\nu_n)]. \quad (4)$$

where  $\Omega_0 = 2 \sum_{\mathbf{k}} \ln(1 + e^{-\beta \xi_{\mathbf{k}}})$  is the non-interacting thermodynamic potential and  $\xi_{\mathbf{k}} = \epsilon_{\mathbf{k}} - \mu$ . The many-body vertex function,  $\Gamma_0(\mathbf{q}, i\nu_n)$ , for bosonic Matsubara frequencies  $\nu_n = 2n\pi/\beta$ , is given by

$$\Gamma_0^{-1}(\mathbf{q}, i\nu_n) = \sum_{\mathbf{k}} \left[ \frac{1 - f(\xi_{\mathbf{k}}) - f(\xi_{\mathbf{k}+\mathbf{q}})}{i\nu_n - \xi_{\mathbf{k}+\mathbf{q}} - \xi_{\mathbf{k}}} + \frac{1}{2\epsilon_{\mathbf{k}} + \varepsilon_B} \right] \quad (5)$$

where we have defined the Fermi distribution  $f(x) = 1/(e^{\beta x} + 1)$ . The system can be viewed as a non-interacting mixture of fermions and pairs. We can analytically continue the Matsubara summation of the bosonic frequencies and find the contribution to the pairing fluctuations, writing the thermodynamic potential as  $\Omega = \Omega_0 + \Omega_{\text{GF}}$ ,

$$\Omega_{\text{GF}} = - \sum_{\mathbf{q}} \int_{-\infty}^{+\infty} \frac{d\omega}{\pi} b(\omega) \text{Im} \ln [-\Gamma_0^{-1}(\mathbf{q}, \omega + i0^+)], \quad (6)$$

where  $b(\omega) = 1/(e^{\beta\omega} - 1)$ . The pressure equation of state is found from the thermodynamic potential for a given

temperature  $T$  and binding energy  $\varepsilon_B$  by  $\Omega = -PV$ , where  $V$  is the volume of the system, and the density equation of state is found by satisfying  $n = -\partial\Omega/\partial\mu$ . The dimensionless pressure equation of state is defined,

$$\frac{P\lambda_T^2}{k_B T} = f_p \left( \frac{\mu}{k_B T} \right) \quad (7)$$

where the thermal wavelength is  $\lambda_T = \sqrt{2\pi\hbar^2/(Mk_B T)}$ , and pressure equation of state is related to the density through  $f_n = \partial f_p / \partial(\beta\mu)$ . This derivation of the thermodynamic potential and calculation of the density equation of state is equivalent to taking the  $T$ -matrix approximation with bare fermionic Green functions in the truncated Schwinger-Dyson equations [52]. For this reason, the above NSR approach is alternatively termed as the non-self-consistent  $T$ -matrix approximation.

The NSR equation of state can be considered against other  $T$ -matrix schemes such as the Luttinger-Ward theory, which is a fully self-consistent calculation of the many-body Green's function and we will refer to as  $GG$  theory [31, 37, 53]. The NSR method in two-dimensions has been found to underestimate the density when compared to current experimental results and  $GG$  theory [31], for the calculation of the hydrodynamic equations the NSR method is advantageous over other  $T$ -matrix schemes as it allows for the calculation of the thermodynamic properties and collective modes at a fixed  $\beta\mu$  and  $\beta\varepsilon_B$ .

## B. Virial expansion

In the high temperature and weakly interacting limits we calculate the equation of state through the virial expansion, where the thermodynamic potential is expanded in powers of the fugacity,  $z = e^{\beta\mu}$  [43]. This allows for an exact calculation of the thermodynamic properties and the breathing mode. It is straight forward to calculate the high temperature regime through the virial expansion, here we present some details of the calculation of the virial coefficients and densities and further reading can be found in Refs. [36, 43, 54, 55].

Let us consider the virial expansion up to third order, the pressure and density equations of state are

$$f_p = \int_0^\infty dt \ln [1 + ze^{-t}] + \Delta b_2 z^2 + \Delta b_3 z^3 + \dots, \\ f_n = \frac{\partial f_p}{\partial \beta\mu} = \ln [1 + z] + 2\Delta b_2 z^2 + 3\Delta b_3 z^3 + \dots, \quad (8)$$

where  $\Delta b_2$  and  $\Delta b_3$  are the second and third virial coefficients respectively. It is important to note that the virial coefficients are functions of the dimensionless binding energy,  $\beta\varepsilon_B$ , only. We calculate the second order virial coefficient through the relation [36],

$$\Delta b_2 = e^{\beta\varepsilon_B} - \int_0^\infty \frac{dp}{p} \frac{e^{p^2}}{\pi^2 + \ln [p^2/(\beta\varepsilon_B)]}, \quad (9)$$

and the third order coefficient,  $\Delta b_3$ , has been tabulated as a function of  $\beta\varepsilon_B$  in the range  $\beta\varepsilon_B = (0.001, 10.0)$  [12]. The third order expansion of the pressure and density equations of state are divergent when  $z > 1$ , however through a Páde expansion we may overcome this divergence and expand the regime of the equation of state [56]. Specifically the third order reduced pressure through the Páde expansion is,

$$\frac{P}{P_0} = \frac{1 + \left( b_2^{(1)} + \Delta b_2 - \Delta b_3 / \Delta b_2 \right) e^{\beta\mu} + \dots}{1 + \left( b_2^{(1)} - \Delta b_3 / \Delta b_2 \right) e^{\beta\mu} + \dots} \quad (10)$$

where  $b_2^{(1)} = -1/4$  is the second virial coefficient of an ideal 2D Fermi gas and  $P_0 = -2\pi\lambda_T^{-4} \text{Li}_2(-e^{\beta\mu})$  is the ideal pressure with  $\text{Li}_2(x)$  being the polylogarithm. Although the expansion can be found for any value of the fugacity,  $z$ , and the pressure equation of state no longer diverges, there is no *a priori* reason for the expansion to be physically correct. We note that the determination of higher order terms such as  $e^{2\beta\mu}$  requires knowledge of the fourth and fifth virial coefficients.

The virial expansion is valid in the BEC limit where  $\varepsilon_B$  becomes large and the chemical potential approaches  $\mu \rightarrow -\varepsilon_B/2$ . In this limit the virial expansion would appear to be valid in the limit  $T \rightarrow 0$ , however the dimer contribution to the virial coefficients dominates and the expansion of the thermodynamic potential in this regime should be in terms of a shifted fugacity,  $z^{(\text{Bose})} = e^{\beta\varepsilon_B/2} z$ , the criterion for the validity of the expansion then becomes  $\mu < -\varepsilon_B/2$ . In this expansion the virial coefficients correspond to  $b_j^{(\text{Bose})} = e^{-j\beta\varepsilon_B/2} b_j$ . An expansion of the Bose thermodynamic potential, taking the effective dimer-dimer scattering length  $a_{dd} \simeq 0.56a_{2D}$  [49, 57], is also dominated by the large binding energy and has the same behavior in the BEC regime.

## C. The pressure equation of state

The pressure equation of state plays a key role in determining the collective modes of a strongly interacting Fermi gas in the hydrodynamic regime [28]. To illustrate the structure of the equation of state before we calculate the collective modes we plot the reduced pressure equation of state,  $P/P_0$ , in Fig. 1. We show the pressure equation of state for the NSR (red solid) and  $GG$  (blue dotted)  $T$ -matrix theories, the second (purple long-dashed) and third (black short dashed) virial expansions, and the Páde expansion (green dot dashed) of the third order virial for interaction strengths of  $\beta\varepsilon_B = 0.5$  and  $\beta\varepsilon_B = 1.0$ , as a function of the reduced chemical potential,  $\beta\mu$ . As has been discussed in Refs. [37, 51] the equation of state exhibits a non-trivial maximum as the temperature reduces ( $\beta\mu \rightarrow \infty$ ), and in Fig. 1 we see that the pressure equations of state for the NSR and  $GG$  theories begin to reduce at low temperatures. The pressure is underestimated by the NSR when compared to the  $GG$

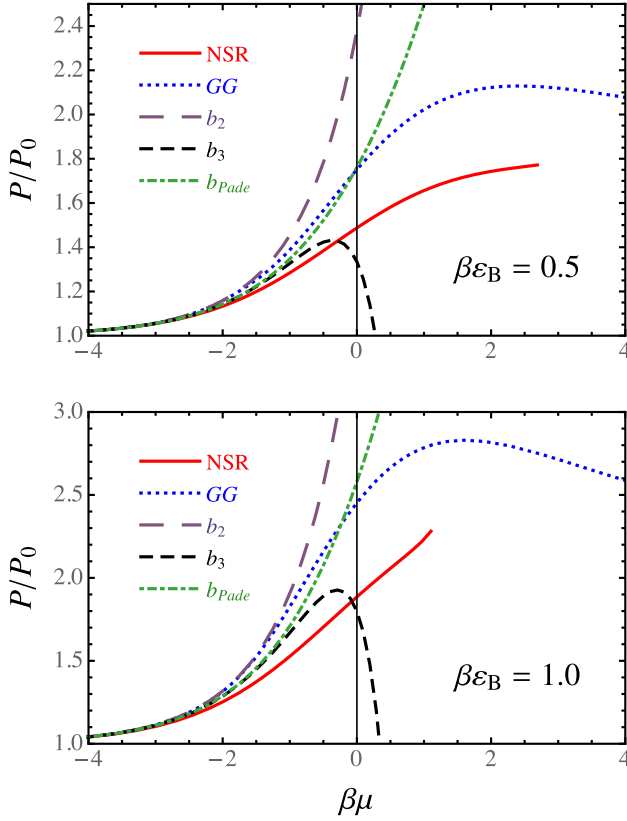


Figure 1. (color online). The pressure equation of state, in units of the pressure of an ideal Fermi gas  $P_0$ , as a function of the chemical potential at interaction strengths  $\beta\epsilon_B = 0.5$  and  $\beta\epsilon_B = 1.0$  for the NSR (red solid) and  $GG$  (blue dotted)  $T$ -matrix theories, second (purple long-dashed) and third (black dashed) order virial expansions, and the Pade expansion of the third order virial (green dot-dashed).

and virial expansions. The virial expansions do not have the non-trivial dependence on the temperature, and are incorrect in the low temperature regime ( $\beta\mu \rightarrow \infty$ ) where they overestimate the pressure.

We see in Fig. 1 that the NSR theory breaks down at higher temperatures compared to the  $GG$  theory, making the range of temperatures in the calculation of the breathing mode smaller. It is well known that two-dimensional  $T$ -matrix theories cannot predict a transition to superfluidity due to the breakdown of long-range order at any finite temperature, however the NSR theory still suffers from a loss of accuracy as the temperature is reduced and the chemical potential approaches half the binding energy (for a detailed analysis see Ref. [1, 38]). The  $GG$  theory is more robust and the equation of state can be calculated to lower temperatures, however we focus on calculating the collective modes of the two-dimensional gas through the NSR theory as we can calculate the numerical derivatives with respect to  $\beta\epsilon_B$  and  $\beta\mu$ . The equation of state for the  $GG$  theory is found for a fixed  $\beta\epsilon_B$  and we iteratively find a chemical potential that satisfies the corresponding number equation, mak-

ing the calculation of thermodynamic properties heavily reliant on numerical interpolation. We expect from previous studies that the breathing mode will not be too sensitive to the equation of state [58, 59]. Therefore, the use of the equations of state from different theories will not greatly affect the calculation of the breathing mode frequency and the *qualitative* behavior of the breathing mode could be captured.

### III. HYDRODYNAMIC FRAMEWORK

We follow the work of [27, 28] to calculate the finite temperature collective modes of a two-dimensional Fermi gas trapped in a harmonic potential  $V_{\text{tr}} = \frac{1}{2}M\omega_0^2 r^2$ . From the equation of state of the homogeneous 2D Fermi gas and the local density approximation, the collective modes of a Fermi gas can be found for frequency  $\omega$  and temperature  $T$  by minimizing a variational action, which in terms of the normal state displacement fields  $\mathbf{u}_n(\mathbf{r})$  takes the form [29],

$$S^{(2)} = \frac{1}{2} \int d\mathbf{r} \left[ \omega^2 \rho_0 \mathbf{u}_n(\mathbf{r})^2 - \frac{1}{\rho_0} \left( \frac{\partial P}{\partial \rho} \right)_{\bar{s}} (\delta \rho)^2 - 2\rho_0 \left( \frac{\partial T}{\partial \rho} \right)_{\bar{s}} \delta \rho \delta \bar{s} - \rho_0 \left( \frac{\partial T}{\partial \bar{s}} \right)_{\bar{s}} (\delta \bar{s})^2 \right]. \quad (11)$$

We define the total mass density at equilibrium,  $\rho(\mathbf{r}) \equiv M n(\mathbf{r}) = \rho_0$ , the local pressure  $P(\mathbf{r}) = P_0$ , the entropy per unit mass  $\bar{s}(\mathbf{r}) \equiv s/\rho = \bar{s}_0$ , and  $\delta \rho(\mathbf{r}) = -\nabla \cdot (\rho_0 \mathbf{u}_n)$  and  $\delta \bar{s}(\mathbf{r}) = -\mathbf{u}_n \cdot \nabla \bar{s}_0$  are the density and entropy fluctuations, respectively. Taking the variation of the action with respect to  $\mathbf{u}_n$  we arrive at

$$\omega^2 \rho_0 \mathbf{u}_n + \nabla \left[ \rho_0 \left( \frac{\partial P}{\partial \rho} \right)_{\bar{s}} (\nabla \cdot \mathbf{u}_n) \right] + \nabla \cdot (\rho_0 \mathbf{u}_n) \frac{\nabla V_{\text{tr}}}{M} + \nabla [\nabla P_0 \cdot \mathbf{u}_n] = 0, \quad (12)$$

which is Euler's equation as first derived in Re. [26]. For an untrapped gas the solution of Eq. (12) is a wave vector  $q$ , with dispersion  $\omega = c_n q$  and  $c_n$  is the speed of sound,

$$c_n = \sqrt{\frac{1}{m} \left( \frac{\partial P}{\partial n} \right)_{\bar{s}}}, \quad (13)$$

where

$$\begin{aligned} n \left( \frac{\partial P}{\partial n} \right)_{\bar{s}} &= n \left( \frac{\partial P}{\partial n} \right)_s + s \left( \frac{\partial P}{\partial s} \right)_n, \\ &= n \frac{\partial(P, s)/\partial(\mu, T)}{\partial(n, s)/\partial(\mu, T)} + s \frac{\partial(P, n)/\partial(\mu, T)}{\partial(s, n)/\partial(\mu, T)}, \\ &= \frac{n(P_\mu s_T - P_T s_\mu) - s(P_\mu n_T - P_T n_\mu)}{(n_\mu s_T - n_T s_\mu)}. \end{aligned} \quad (14)$$

For convenience we use the shorthand notation  $P_\mu \equiv (\partial P / \partial \mu)_T$ ,  $s_T \equiv (\partial s / \partial T)_\mu$ , etc, and in dimensionless

form we obtain

$$\left(\frac{\partial P}{\partial n}\right)_{\bar{s}} = k_B T \frac{(\tilde{P}_\mu \tilde{s}_T - \tilde{P}_T \tilde{s}_\mu) - \tilde{s}(\tilde{P}_\mu \tilde{n}_T - \tilde{P}_T \tilde{n}_\mu)}{(\tilde{n}_\mu \tilde{s}_T - \tilde{n}_T \tilde{s}_\mu)}. \quad (15)$$

All of the thermodynamic quantities can then be found from the pressure equation of state by taking partial derivatives with respect to the reduced chemical potential,  $\beta\mu$  and interaction strength,  $\beta\varepsilon_B$ .

We calculate the thermodynamic potential of a harmonically trapped gas through the local density approximation,  $\mu(r) = \mu - V_{\text{tr}}(r)$ , and write the local pressure and number density using the universal functions,

$$P(r) = \frac{k_B T}{\lambda_T^2} f_p \left[ \frac{\mu(r)}{k_B T} \right], \quad n(r) = \frac{1}{\lambda_T^2} f_n \left[ \frac{\mu(r)}{k_B T} \right], \quad (16)$$

where the local chemical potential is  $\mu(r)$  and the Fermi temperature is defined as,

$$k_B T_F = \hbar(2N\omega_0^2)^{1/2}. \quad (17)$$

Using the number equation  $N = \int dr n(r)$  we relate the reduced chemical potential  $\beta\mu$  to the reduced temperature in the trap  $T/T_F$  by,

$$\frac{T}{T_F} = \left[ 2 \int_0^\infty dy f_n(\beta\mu - y) \right]^{-1/2}. \quad (18)$$

For a given trap temperature we need the dimensionless chemical potential,  $\beta\mu_c$ , which satisfies Eq. (18) (as temperature reduces  $\beta\mu_c \rightarrow \infty$ ). To minimize the action in Eq. (11) we expand the displacement field in a variational (polynomial) basis by using the following ansatz,

$$\mathbf{u}_n(\mathbf{r}) = \sum_{n=0}^{N_\perp} A_n r^{n+1}, \quad (19)$$

where we can increase the precision of the variational calculation by increasing the number of basis functions,  $N_\perp$ . Expanding the action we get,

$$S_n^{(2)} = \frac{1}{2} [A_0^*, \dots, A_{N_\perp}^*] \mathbf{A}(\omega) [A_0, \dots, A_{N_\perp}]^T, \quad (20)$$

where  $\mathbf{A}(\omega)$  is a  $N_\perp \times N_\perp$  matrix,

$$A_{nm}(\omega) = \omega^2 M_{nm} - K_{nm}. \quad (21)$$

Here we have defined the weighted mass moments,  $\mathbf{M} = M_{nm}$ , and spring constants,  $\mathbf{K} = K_{nm}$  given in Appendix A. To find the mode frequencies we need to solve the matrix equation,

$$\mathbf{A}(\tilde{\omega}) \mathbf{x} = 0, \quad (22)$$

where the vector of displacement fields are given by,  $\mathbf{x} = [A_0, \dots, A_n, \dots]^T$ , and we write the matrix  $\mathbf{A}(\tilde{\omega}) = \mathbf{M}\tilde{\omega}^2 - \mathbf{K}$  in terms of the dimensionless frequency  $\tilde{\omega} = \omega/\omega_0$ . The details of this calculation are given in Appendix B. The breathing mode is the lowest frequency found from solving Eq. (22). The variational result converges quickly, where the  $n = 0$  giving the most significant contribution.

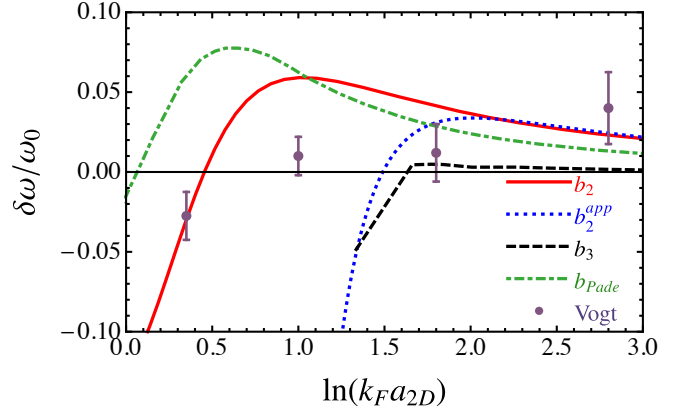


Figure 2. (color online). The frequency shift of the breathing mode from the scale invariant value,  $\delta\omega = \omega - 2\omega_0$ , at temperature  $T/T_F = 0.42$  as a function of interaction strength  $\ln(k_F a_{2D})$  for the second order virial (red solid), dilute limit second order virial (blue dotted) [25], third order virial (black dashed), Páde virial expansion (green dot-dashed), and experimental results from Ref. [19] (symbols).

## IV. RESULTS AND DISCUSSION

We now turn to examining the breathing mode at finite temperature. We first consider the results obtained by using the virial expansion approach, contrasted to the experimental data of Ref. [19] and the previous virial results of Ref. [25], and then compare the predictions from the different  $T$ -matrix theories. We finally check the breathing mode in the high temperature regime, where the virial expansion is more reliable and we examine the role of pairing at high temperature.

### A. Virial comparison

In Fig. 2 we compare the frequency shift of the breathing mode from the scale invariant value,  $\delta\omega = \omega - 2\omega_0$ , as a function of interaction strength  $\ln(k_F a_{2D})$  on the BCS side for the virial expansion at a temperature of  $T/T_F = 0.42$ . The use of virial expansion at this (low) temperature could be questionable. However, we present the comparison for the purpose of making connect to the experimental measurement [19] and also making contact with the previous virial expansion study [25]. We compute the breathing mode using the second order virial (red solid), third order virial (black dashed), Páde expansion of the third order virial (green-dot dashed), a dilute expansion of the second order virial as found in Ref. [25] (blue dotted), and the experimental results of Ref. [19] (symbols).

The breathing mode found in Ref [25] is calculated from a second order expansion of the equation of state, however the authors *further* approximate the trap density and the speed of sound in the dilute limit, computing

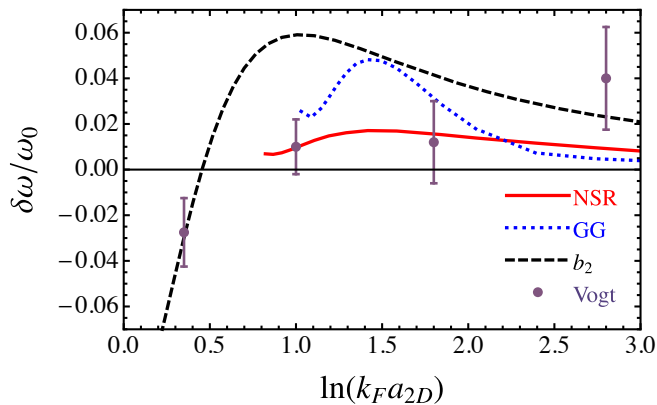


Figure 3. (color online). The frequency shift of the breathing mode from the scale invariant value,  $\delta\omega = \omega - 2\omega_0$ , at temperature  $T/T_F = 0.42$  as a function of interaction strength  $\ln(k_F a_{2D})$  for the NSR (red solid) and  $GG$  (blue dotted)  $T$ -matrix theories, second order virial (black dashed), and experimental results from Ref. [19] (symbols).

the breathing mode to be

$$\frac{\omega^2}{4\omega_0^2} = 1 - \frac{1}{8} \frac{T_F^2 \varepsilon_B^2}{T^4} \frac{\partial^2 \Delta b_2}{\partial (\beta \varepsilon_B)^2}, \quad (23)$$

where  $\Delta b_2(\beta \varepsilon_B)$  is given by Eq. (9). We see that our second order virial calculation extends to stronger interaction strengths before lowering, however we emphasize that at this temperature the virial expansion is not accurate and the results should be treated as qualitative only. We see that at the reduced trap temperature of  $T/T_F = 0.42$  over the interaction regime the virial expansions of second order, third order, and Páde expansion are not the same. This can be understood by looking at the pressure equation of state in Fig. 1, the critical chemical potential  $\beta\mu_c$  needed to determine the trap temperature in Eq. (18) is in the regime where the second and third expansions differ significantly, and where the third order is diverging. Although we can calculate the thermodynamic properties for the speed of sound within the virial expansion, for this temperature and interaction regime, the breathing mode results are only qualitative.

### B. $T$ -matrix results at low temperature

The  $T$ -matrix theories take into account the many-body effects and pairing fluctuations, extending the equation of state found through the virial expansions to lower temperatures. In Fig. 3 we compare the frequency shifts of the breathing mode  $\delta\omega = \omega - 2\omega_0$  at a reduced temperature of  $T/T_F = 0.42$  obtained by the NSR (red solid) and self-consistent  $GG$   $T$ -matrix (blue dotted) theories, second order virial expansion (black dashed), and also compare them to the experimental work of Ref. [19] (symbols). For each of the frequency shifts there is a maximum, and as the interaction becomes stronger the

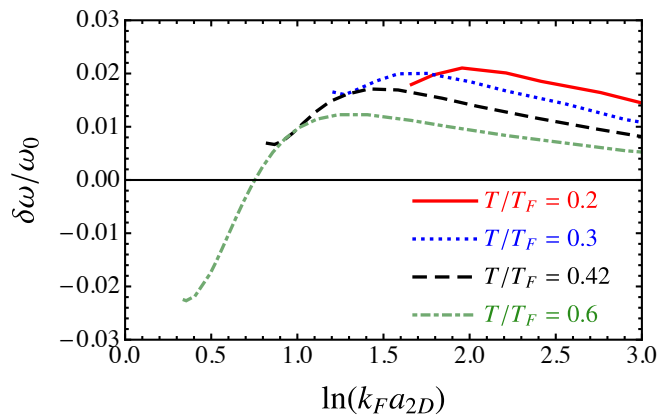


Figure 4. (color online). The frequency shift of the breathing mode,  $\delta\omega = \omega - 2\omega_0$ , as a function of interaction strength  $\ln(k_F a_{2D})$  for the NSR  $T$ -matrix at temperature  $T/T_F = 0.2$  (red solid),  $T/T_F = 0.3$  (blue dotted),  $T/T_F = 0.42$  (black dashed), and  $T/T_F = 0.6$  (green dot-dashed).

frequency shift reduces towards  $\delta\omega = 0$ , as is seen in the experimental results of Ref. [19]. The difference between the NSR and  $GG$  theories could be due to the fact that the NSR approach underestimates the pressure. Although the second order virial expansion is not reliable in this regime, the qualitative behavior is similar to the NSR and  $GG$  theories.

We see in Fig. 3 that the NSR breathing mode breaks down for an interaction of  $\ln(k_F a_{2D}) \simeq 0.9$  where the critical chemical potential needed for the reduced trap temperature is too large within the  $T$ -matrix theory. The  $GG$  frequency shift breaks down at  $\ln(k_F a_{2D}) \simeq 1.0$ , and is different to the breakdown of the NSR theory. For stronger interactions the numerical noise in the calculation of thermodynamic properties is too large to accurately determine the speed of sound.

In Fig. 4 we consider how the frequency shift of the breathing mode behaves as a function of temperature using the NSR theory, specifically for  $T/T_F = 0.2$  (red solid),  $T/T_F = 0.3$  (blue dotted),  $T/T_F = 0.42$  (black dashed), and  $T/T_F = 0.6$  (green dot-dashed). As temperature decreases the frequency shift increases, indicating that as temperature is reduced the breathing mode anomaly will be larger. We find that the range of validity of the NSR calculation reduces with decreasing temperature and the NSR theory also breaks down at higher temperatures as we increase the binding energy. The frequency shift at all temperatures considered has a maximum value that lowers as interaction strength increases, a result consistent in all of the theories and temperatures considered in this work. Therefore, we believe that this will be qualitatively true for further experimental checks at finite temperature. However, for temperatures below  $T/T_F = 0.2$  it is not clear if the frequency shift will lower or be positive over the whole BEC-BCS crossover.



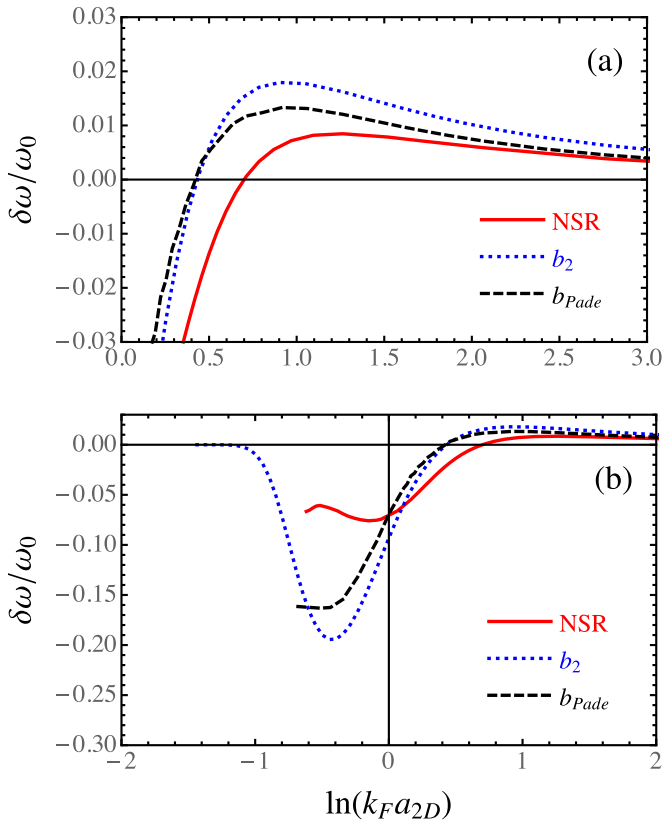


Figure 5. (color online). The frequency shift of the breathing mode,  $\delta\omega = \omega - 2\omega_0$ , at temperature  $T/T_F = 0.8$  as a function of interaction strength  $\ln(k_F a_{2D})$  for the NSR  $T$ -matrix (red solid), second order virial expansion (blue dotted), and third order Páde virial expansion (black dashed), for (a) the BCS regime and (b) the BEC-BCS crossover.

### C. High temperature limit

For the reduced trap temperature of  $T/T_F = 0.6$  in Fig. 4 the interaction range of validity is increased and we see that the frequency shift becomes negative before the NSR results break down. This increased range of validity allows us to examine the breathing mode and the effects of pairing at temperatures far above the critical temperature. In two dimensions the role of pairing in the high temperature regime is a widely discussed area of research [10, 60].

The NSR and virial expansions are valid for a wide range of interactions at high temperatures and we can cover the BEC-BCS crossover, where we also *assume* that the hydrodynamic equations are still valid [61]. In Fig. 5 we calculate the breathing mode shift for a temperature of  $T/T_F = 0.8$ , with the NSR theory (red solid), second order virial (blue dotted), and Páde expansion (black dashed). Figure 5(a) shows that in the BCS limit the frequency shift is approaching the scale invariant result of  $\delta\omega = 0$ . As we approach the strongly interacting regime, the frequency shift has a maximum value and then tends negative, and the breathing mode anomaly seems to be

weakened at first glance. However, expanding the interaction range and looking at Fig. 5(b) we see that the NSR, virial, and Páde expansion predict a significant negative shift in the strongly interacting regime. The NSR theory finds a breathing mode shift of 4% and the second order virial expansion 10%. Going deeper to the BEC side the NSR and Páde theories break down for  $\ln(k_F a_{2D}) \simeq -0.6$ , and the second order virial expansion finds that the breathing mode approaches the scale invariant value of  $2\omega_0$  by  $\ln(k_F a_{2D}) \simeq -1$ .

We would like to argue that the significant down-shift of the breathing mode in the strongly interacting regime is due to pairing effects. On the BEC side of the strongly interacting regime (i.e.,  $-1 < \ln(k_F a_{2D}) < 0$  with  $\beta\mu < 0$ ), the two-body pairing is captured by the second order virial expansion or the Páde expansion. Here, it is known that pairing above  $T_c$  is without a Fermi surface [5], and therefore is not associated with the pseudogap. In contrast, on the BCS side of the strongly interacting regime, the NSR theory predicts a chemical potential of  $\beta\mu \simeq 0$ , and pair formation is a many-body effect. Any possible experimental observations of the predicted down-shift of the breathing mode frequency are therefore of important for understanding the role of pairing in two-dimensional Fermi systems.

## V. CONCLUSION

In summary we have investigated the behavior of the breathing mode at finite temperature for a strongly interacting 2D Fermi gas at the BEC-BCS crossover. Using the equation of state found from the NSR and self-consistent  $T$ -matrix theories as well as the virial expansion at different orders for a homogenous Fermi gas, we have predicted the breathing mode at finite temperature of a trapped gas through the local density approximation and a variational approach to the hydrodynamic Euler equation. The use of different theories for a strongly interacting Fermi gas enable us to paint a broad and qualitative picture of the breathing mode at finite temperature. Both  $T$ -matrix theories and virial expansions consistently show the sensitivity of the quantum anomaly on the temperature and interaction strength, that is, the frequency shift of the breathing mode is sensitively dependent on temperature and interaction.

On the BCS side, we have predicted that the breathing mode frequency reduces towards the scale invariant value of  $2\omega_0$  as temperature increases and, the quantum anomaly is more prominent at low temperatures, as one may anticipate. At the typical interaction strength  $\ln(k_F a_{2D}) \simeq 2$ , the frequency shift predicted by the NSR approach is at the level of 1% for temperature up to  $0.6T_F$ . Considering the high experimental resolution for frequency measurements with cold-atoms, which is about 0.1% [62], this shift is significant enough to be resolved in future experiments.

In the strongly interacting regime, we have confirmed

that a significant negative frequency shift at high temperatures, peaking near  $\ln(k_F a_{2D}) \simeq -0.4$ , as predicted by both NSR and virial expansion theories. This may be due to the strong pairing effects included in the calculations of the homogeneous equation of state. We note that, a down-shift of the breathing mode frequency, below the scale invariant value, was also predicted by Chafin and Schäfer using the second-order virial expansion at  $T = 0.42T_F$  [25]. Our more systematic virial expansion studies, beyond the second order, unambiguously confirm their finding and establish the qualitative behavior of the breathing mode frequency at high temperature at the whole BEC-BCS crossover.

### ACKNOWLEDGMENTS

We would like to thank T. Peppler, P. Dyke, and C. Vale for their useful discussions. This research was supported under Australian Research Council's Discovery Projects funding scheme (project numbers DP140100637, DP140103231, and DP170104008) and Future Fellowships funding scheme (project numbers FT130100815 and FT140100003).

### Appendix A: Variational approach

Here we consider in more detail the expressions for the weighted mass moments,  $M_{nm}$ , and spring constants,  $K_{nm}$ . We present a detailed derivation of the weighted mass moments as this will be instructive to the choice of units. The weighted mass moments,  $M_{nm}$ , arise from the following action term

$$\omega^2 \int d\mathbf{r} \rho_0 \mathbf{u}_n^2 = A_n A_m \omega^2 \int d\mathbf{r} \rho_0(r) \tilde{r}^{n+m+2}, \quad (\text{A1})$$

where we have denoted  $\tilde{r} \equiv r/R_{\text{TF}}$  and  $R_{\text{TF}}^2 = 2k_B T_F / (m\omega_0^2)$  is the Thomas-Fermi temperature for a zero-temperature noninteracting Fermi gas. Recalling that within the local density approximation, we have,  $\rho_0(r) = M n_0(r) = M \lambda_T^{-2} f_n[(\mu - V_{\text{tr}}(r))/k_B T]$ , thus

$$\begin{aligned} \int d\mathbf{r} \rho_0(r) \tilde{r}^k &= \frac{R_F^2 M}{\lambda_T^2} \int d\tilde{\mathbf{r}} f_n \left( \beta\mu - \frac{M\omega_0^2 r^2}{2k_B T} \right) \tilde{r}^k, \\ &= \frac{R_F^2 M 2\pi}{\lambda_T^2} \int d\tilde{r} f_n \left( \beta\mu - \frac{\tilde{r}^2}{T/T_F} \right) \tilde{r}^{k+1}. \end{aligned} \quad (\text{A2})$$

There is a constant here that will set to 1 as it appears in all of the equations. As a result of the above calculation we can tie the reduced temperature  $T/T_F$  of the system to a given  $\mu/k_B T$  by using the number equation for  $N$

atoms,  $MN = \int d\mathbf{r} \rho_0(r)$ , that is

$$\begin{aligned} N \lambda_T^2 &= \int d\mathbf{r} f_n \left( \beta\mu - \frac{M\omega_0^2 r^2}{2k_B T} \right), \\ \frac{N \lambda_T^2}{R_{\text{TF}}^2 2\pi} &= \int d\tilde{r} \tilde{r} f_n \left( \beta\mu - \frac{\tilde{r}^2}{T/T_F} \right). \end{aligned} \quad (\text{A3})$$

Using the fact that  $\lambda_T^2 = 2\pi\hbar/(Mk_B T)$  and  $k_B T_F = \hbar(2N\omega_0^2)^{1/2}$ , we have

$$\frac{T_F}{4T} = \int d\tilde{r} \tilde{r} f_n \left( \beta\mu - \frac{\tilde{r}^2}{T/T_F} \right), \quad (\text{A4})$$

changing coordinates to  $y = \tilde{r}^2/(T/T_F)$  gives in total,

$$\frac{T}{T_F} = \left[ 2 \int_0^\infty dy f_n(\beta\mu - y) \right]^{-1/2} \quad (\text{A5})$$

This definition allows us to find a reduced temperature for the trapped system for a given  $\beta\mu$  in the homogeneous system.

The spring constant

$$\begin{aligned} (\nabla \rho_0 \cdot \mathbf{u}_n) \left( \frac{\nabla V_{\text{tr}}}{M} \cdot \mathbf{u}_n \right) &= \frac{\partial \rho_0}{\partial r} A_n \tilde{r}^{n+1} r A_m \omega_\perp \tilde{r}^{m+1} r \\ \rho_0 (\nabla \cdot \mathbf{u}_n) \left( \frac{\nabla V_{\text{tr}}}{M} \cdot \mathbf{u}_n \right) &= \rho_0 \frac{n+2}{R_{\text{TF}}} \tilde{r}^n A_n \omega_\perp^2 r \tilde{r}^{m+1} A_m \\ \rho_0 \left( \frac{\nabla V_{\text{tr}}}{M} \cdot \mathbf{u}_n \right) (\nabla \cdot \mathbf{u}_n) &= \rho_0 A_n \omega_0^2 r \tilde{r}^{n+1} A_n \frac{m+2}{R_{\text{TF}}} \tilde{r}^m \\ c_n (\nabla \cdot \mathbf{u}_n)^2 &= c_n \frac{n+2}{R_{\text{TF}}} \frac{m+2}{R_{\text{TF}}} r^n r^m A_n A_m, \end{aligned} \quad (\text{A6})$$

The spring constants cancel leaving only Eq. (A6) to calculate,

$$\begin{aligned} K_{nm} &= (n+2)(m+2) \frac{M\omega_0^2}{2k_B T_F} \int d\mathbf{r} \left[ n_0 \left( \frac{\partial P}{\partial n} \right)_{\tilde{s}} \right] \tilde{r}^{n+m}, \\ &= (n+2)(m+2) \frac{M\omega_0^2 R_F^2}{2k_B T_F \lambda_T^2} k_B T \\ &\quad \times \int d\mathbf{r} f_n \left( \beta\mu - \frac{M\omega_0^2 r^2}{2k_B T} \right) \left( \frac{\partial P}{\partial n} \right)_{\tilde{s}} \tilde{r}^{n+m}, \\ &= (n+2)(m+2) \frac{M\omega_0^2 R_F^2 \pi}{\lambda_T^2} \frac{T}{T_F} \\ &\quad \times \int_0^\infty d\tilde{r} f_n \left( \beta\mu - \frac{\tilde{r}^2}{T/T_F} \right) \left( \frac{\partial P}{\partial n} \right)_{\tilde{s}} \tilde{r}^{n+m+1}. \end{aligned} \quad (\text{A7})$$

### Appendix B: Solving for $\det \mathbf{A}(\tilde{\omega}) = 0$

In order to solve the matrix equation  $\mathbf{A}(\tilde{\omega}) \mathbf{x} = 0$ , where the vector of displacement fields is,  $\mathbf{x} = [A_0, \dots, A_n, \dots]^T$ , we expand the matrix  $\mathbf{A}(\tilde{\omega}) = \mathbf{M}\tilde{\omega}^2 -$



$\mathbf{K}$  to find the eigenvalues. Here,  $\mathbf{M}$  and  $\mathbf{K}$  are the matrices of the reduced weighted mass moments and the spring constants, respectively. The matrix  $\mathbf{M}$  can be written as a product of a lower triangular matrix  $\mathbf{L}$ , its conjugate transpose, and a diagonal matrix  $\mathbf{D}$ ,

$$\mathbf{M} = \mathbf{L} \cdot \mathbf{D} \cdot \mathbf{L}^T. \quad (\text{B1})$$

In terms of this decomposition, the matrix equation  $\mathbf{A}(\tilde{\omega}) \mathbf{x} = 0$  is written as,

$$[\mathbf{D}^{-1} \cdot \mathbf{L}^{-1} \cdot \mathbf{K} \cdot (\mathbf{L}^{-1})^T] \mathbf{L}^T \mathbf{x} = \tilde{\omega}^2 \mathbf{L}^T \mathbf{x}. \quad (\text{B2})$$

We see that the eigenvalues of the positive definite matrix,  $[\mathbf{D}^{-1} \cdot \mathbf{L}^{-1} \cdot \mathbf{K} \cdot (\mathbf{L}^{-1})^T]$  are the mode frequencies,  $\tilde{\omega}$ . The displacement field for each eigenvalue can also be calculated similarly, with each eigenstate of the matrix  $[\mathbf{D}^{-1} \cdot \mathbf{L}^{-1} \cdot \mathbf{K} \cdot (\mathbf{L}^{-1})^T]$ . Once the displacement fields for a mode are found, we may calculate its density fluctuation.

- 
- [1] V. M. Loktev, R. M. Quick, and S. G. Sharapov, *Physics Reports* **349**, 1 (2001).
  - [2] P. A. Lee, N. Nagaosa, and X.-G. Wen, *Rev. Mod. Phys.* **78**, 17 (2006).
  - [3] B. Holstein, *American Journal of Physics* **61** (1993).
  - [4] S. K. Adhikari, *American Journal of Physics* **54**, 362 (1986).
  - [5] J. Levinsen and M. M. Parish, in *Annual Review of Cold Atoms and Molecules*, Vol. Volume 3 (WORLD SCIENTIFIC, 2015) pp. 1–75–.
  - [6] A. Turlapov and M. Y. Kagan, *Journal of Physics: Condensed Matter* (2017).
  - [7] L. P. Pitaevskii and A. Rosch, *Phys. Rev. A* **55**, R853 (1997).
  - [8] M. Olshanii, H. Perrin, and V. Lorent, *Phys. Rev. Lett.* **105**, 095302 (2010).
  - [9] F. Werner and Y. Castin, *Phys. Rev. A* **74**, 053604 (2006).
  - [10] M. Feld, B. Frohlich, E. Vogt, M. Koschorreck, and M. Kohl, *Nature* **480**, 75 (2011).
  - [11] V. Makhlov, K. Martinyanov, and A. Turlapov, *Phys. Rev. Lett.* **112**, 045301 (2014).
  - [12] K. Fenech, P. Dyke, T. Peppler, M. G. Lingham, S. Hoinka, H. Hu, and C. J. Vale, *Phys. Rev. Lett.* **116**, 045302 (2016).
  - [13] P. A. Murthy, I. Boettcher, L. Bayha, M. Holzmann, D. Kedar, M. Neidig, M. G. Ries, A. N. Wenz, G. Zürn, and S. Jochim, *Phys. Rev. Lett.* **115**, 010401 (2015).
  - [14] I. Boettcher, L. Bayha, D. Kedar, P. A. Murthy, M. Neidig, M. G. Ries, A. N. Wenz, G. Zürn, S. Jochim, and T. Enss, *Phys. Rev. Lett.* **116**, 045303 (2016).
  - [15] F. Chevy, V. Bretin, P. Rosenbusch, K. W. Madison, and J. Dalibard, *Phys. Rev. Lett.* **88**, 250402 (2002).
  - [16] B. Jackson and E. Zaremba, *Phys. Rev. Lett.* **89**, 150402 (2002).
  - [17] S. P. Rath, T. Yefsah, K. J. Günter, M. Cheneau, R. Desbuquois, M. Holzmann, W. Krauth, and J. Dalibard, *Phys. Rev. A* **82**, 013609 (2010).
  - [18] T. Yefsah, R. Desbuquois, L. Chomaz, K. J. Günter, and J. Dalibard, *Phys. Rev. Lett.* **107**, 130401 (2011).
  - [19] E. Vogt, M. Feld, B. Fröhlich, D. Pertot, M. Koschorreck, and M. Köhl, *Phys. Rev. Lett.* **108**, 070404 (2012).
  - [20] S. K. Baur, E. Vogt, M. Köhl, and G. M. Bruun, *Phys. Rev. A* **87**, 043612 (2013).
  - [21] J. Hofmann, *Phys. Rev. Lett.* **108**, 185303 (2012).
  - [22] E. Taylor and M. Randeria, *Phys. Rev. Lett.* **109**, 135301 (2012).
  - [23] C. Gao and Z. Yu, *Phys. Rev. A* **86**, 043609 (2012).
  - [24] G. Bertaina and S. Giorgini, *Phys. Rev. Lett.* **106**, 110403 (2011).
  - [25] C. Chafin and T. Schäfer, *Phys. Rev. A* **88**, 043636 (2013).
  - [26] A. Griffin, W.-C. Wu, and S. Stringari, *Phys. Rev. Lett.* **78**, 1838 (1997).
  - [27] E. Taylor, H. Hu, X.-J. Liu, and A. Griffin, *Phys. Rev. A* **77**, 033608 (2008).
  - [28] E. Taylor and M. Randeria, *Phys. Rev. Lett.* **109**, 135301 (2012).
  - [29] H. Hu, P. Dyke, C. J. Vale, and X.-J. Liu, *New Journal of Physics* **16**, 083023 (2014).
  - [30] G. De Rosi and S. Stringari, *Phys. Rev. A* **92**, 053617 (2015).
  - [31] B. C. Mulkerin, K. Fenech, P. Dyke, C. J. Vale, X.-J. Liu, and H. Hu, *Phys. Rev. A* **92**, 063636 (2015).
  - [32] C. Gies and D. A. W. Hutchinson, *Phys. Rev. A* **70**, 043606 (2004).
  - [33] X.-J. Liu, H. Hu, and P. D. Drummond, *Phys. Rev. B* **82**, 054524 (2010).
  - [34] V. Pietilä, *Phys. Rev. A* **86**, 023608 (2012).
  - [35] R. Watanabe, S. Tsuchiya, and Y. Ohashi, *Phys. Rev. A* **88**, 013637 (2013).
  - [36] V. Ngampruetikorn, J. Levinsen, and M. M. Parish, *Phys. Rev. Lett.* **111**, 265301 (2013).
  - [37] M. Bauer, M. M. Parish, and T. Enss, *Phys. Rev. Lett.* **112**, 135302 (2014).
  - [38] F. Marsiglio, P. Pieri, A. Perali, F. Palestini, and G. C. Strinati, *Phys. Rev. B* **91**, 054509 (2015).
  - [39] B. C. Mulkerin, L. He, P. Dyke, C. J. Vale, X.-J. Liu, and H. Hu, *ArXiv e-prints* (2017), arXiv:1702.07091 [cond-mat.quant-gas].
  - [40] P. Nozieres and S. Schmitt-Rink, *Journal of Low Temperature Physics* **59**, 195 (1985).
  - [41] M. Randeria, J.-M. Duan, and L.-Y. Shieh, *Physical review letters* **62**, 981 (1989).
  - [42] R. Haussmann, *Zeitschrift für Physik B Condensed Matter*, **91**, 291 (1993).
  - [43] X.-J. Liu, *Physics Reports* **524**, 37 (2013).
  - [44] E. R. Anderson and J. E. Drut, *Phys. Rev. Lett.* **115**, 115301 (2015).
  - [45] C. A. R. Sá de Melo, M. Randeria, and J. R. Engelbrecht, *Phys. Rev. Lett.* **71**, 3202 (1993).

- [46] R. B. Diener, R. Sensarma, and M. Randeria, Phys. Rev. A **77**, 023626 (2008).
- [47] H. Hu, X.-J. Liu, and P. D. Drummond, New Journal of Physics **12**, 063038 (2010).
- [48] S. N. Klimin, J. Tempere, and J. T. Devreese, New Journal of Physics **14**, 103044 (2012).
- [49] L. He, H. Lü, G. Cao, H. Hu, and X.-J. Liu, Phys. Rev. A **92**, 023620 (2015).
- [50] G. Bighin and L. Salasnich, (2015), arXiv:1507.07542.
- [51] B. C. Mulkerin, X.-J. Liu, and H. Hu, Phys. Rev. A **94**, 013610 (2016).
- [52] J. W. Serene, Phys. Rev. B **40**, 10873 (1989).
- [53] R. Haussmann, Phys. Rev. B **49**, 12975 (1994).
- [54] M. Barth and J. Hofmann, Phys. Rev. A **89**, 013614 (2014).
- [55] X. Leyronas, Phys. Rev. A **84**, 053633 (2011).
- [56] H. Hu, X.-J. Liu, and P. D. Drummond, Phys. Rev. A **83**, 063610 (2011).
- [57] L. Salasnich and F. Toigo, Phys. Rev. A **91**, 011604 (2015).
- [58] H. Heiselberg, Phys. Rev. Lett. **93**, 040402 (2004).
- [59] H. Hu, A. Minguzzi, X.-J. Liu, and M. P. Tosi, Phys. Rev. Lett. **93**, 190403 (2004).
- [60] P. A. Murthy, M. Neidig, R. Klemt, L. Bayha, I. Boettcher, T. Enss, M. Holten, G. Zürn, P. M. Preiss, and S. Jochim, ArXiv e-prints (2017), arXiv:1705.10577 [cond-mat.quant-gas].
- [61] M. J. Wright, S. Riedl, A. Altmeyer, C. Kohstall, E. R. S. Guajardo, J. H. Denschlag, and R. Grimm, Phys. Rev. Lett. **99**, 150403 (2007).
- [62] M. K. Tey, L. A. Sidorenkov, E. R. S. Guajardo, R. Grimm, M. J. H. Ku, M. W. Zwiernlein, Y.-H. Hou, L. Pitaevskii, and S. Stringari, Phys. Rev. Lett. **110**, 055303 (2013).